



Vegetation mapping using hierarchical object-based image analysis applied to aerial imagery and lidar data

Kellie A. Uyeda¹  | Kelsey K. Warkentin¹ | Douglas A. Stow¹  | John F. O'Leary¹ | Rachel A. Snavelly¹ | Julie Lambert² | Leslie A. Bolick³ | Kimberly O'Connor⁴ | Bryan Munson⁵ | Andrew C. Loerch¹

¹Department of Geography, San Diego State University, San Diego, CA, USA

²Soil Ecology and Restoration Group, San Diego State University Research Foundation, San Diego, CA, USA

³SPAWAR Systems Center Pacific, San Diego, CA, USA

⁴US Pacific Fleet Natural and Cultural Resources Program, Naval Base Coronado, Coronado, CA, USA

⁵US Naval Facilities Engineering Command Southwest, Naval Base Coronado, Coronado, CA, USA

*Correspondence

Kellie Uyeda, Department of Geography, San Diego State University, San Diego, CA, USA. Email: kuyeda@sdsu.edu

Funding information

This project was funded under agreement (Cooperative Agreement Award No: W9126G-15-2-0034) by the U.S. Army Corps of Engineers.

Co-ordinating Editor: Sebastian Schmidlein

Abstract

Aims: The primary objective of this study is to map the distribution and quantify the cover of vegetation alliances over the entirety of San Clemente Island (SCI). To this end, we develop and evaluate the mapping method of hierarchical object-based classification with a rule-based expert system.

Location: San Clemente Island, California, USA.

Methods: We developed and tested an approach based on hierarchical object-based classification with a rule-based expert system to effectively map vegetation communities on SCI following the Manual of California Vegetation classification system. In this mapping approach, the shrub species defining each vegetation community and non-shrub growth forms were first mapped using aerial imagery and lidar data, then used as input in an automated mapping rule set that incorporates the percent cover rules of a field-based mapping rule set.

Results: The final vegetation map portrays the distribution of 19 vegetation communities across SCI, with the largest areas comprised of California Annual and Perennial Grassland (35%) and three types of coastal sage scrub and maritime succulent scrub, comprising a combined 53% of the area. Map accuracy was assessed to be 79% based on fuzzy methods and 61% with a traditional accuracy assessment. The accuracy of tree identification was assessed to be 81%, but species-level tree accuracy was 45%. **Conclusions:** Semi-automated approaches to vegetation community mapping can produce repeatable maps over large spatial extents that facilitate ecological management efforts. However, some low-statured shrub community types were difficult to differentiate due to patchy canopies of co-occurring species including abundant non-native grasses characteristic of complex disturbance histories. Species-level tree mapping accuracy was low due to the difficulty of identifying species within poorly illuminated canyons, resulting from sub-optimal image acquisition timing.

KEYWORDS

canopy height, coastal sage scrub, Manual of California Vegetation, San Clemente Island, shrubland, southern California vegetation, U.S. National Vegetation Classification, vegetation community, vegetation mapping

1 | INTRODUCTION

Mapping and monitoring vegetation is critically important for a variety of natural resource management goals including maintenance of biodiversity, monitoring of animal habitat, fire management planning, management of non-native plant cover, restoration ecological efforts, and protection of rare, threatened, and endangered plant and animal species (Millington & Alexander, 2000; Faber-Langendoen et al., 2014; Rapinel, Rossignol, Hubert-Moy, Bouzillé, & Bonis, 2018). Automated and semi-automated remote sensing approaches to vegetation mapping have greatly increased the total extent and repeatability of mapping that can be achieved (Corbane et al., 2015). Canopy height information derived from light detection and ranging (lidar) data sets are increasingly used to improve mapping accuracy, particularly in closed-canopy systems such as conifer or hardwood forests (Zhang, Xie, & Selch, 2013; Su et al., 2006). The inclusion of lidar data sets has also been shown to be useful when detecting the cover of individual trees or shrubs (Bork & Su, 2007; Hellesen & Matikainen, 2013; Hulet, Roundy, Petersen, Jensen, & Bunting, 2014). However, a goal of vegetation mapping is often to produce community-level maps rather than simply detecting the presence of a particular growth-form type (Thorne et al., 2004). Low accuracy has been documented for automated approaches to mapping at the community level in heterogeneous, open-canopy shrubland communities (Clark & Kilham, 2016).

Traditional aerial interpretation or field mapping techniques for vegetation mapping are commonly based on a field-based classification key made up of a series of species-specific percent cover rules that define each community type (Sawyer, Keeler-Wolf, & Evens, 2009). Community types obtained by following field-based keys often do not match exactly with the results from statistically based automated mapping systems, particularly when the percent cover threshold for a given community type is less than majority cover (Yu et al., 2006). Without species-specific information for cover, it is difficult to apply field-based mapping rules in a semi-automated mapping system. While it may be possible to correctly map homogeneous closed-canopy community types, the tasks of delineating appropriate boundaries and assigning the correct class are more difficult for heterogeneous, open-canopy community types. Shrublands can be naturally open-canopy systems, but shrub cover can also decline due to disturbances such as grazing or fire (Westman & O'Leary, 1986). These disturbed, open-canopy shrublands are often particularly in need of community-level mapping to support ecological management efforts.

San Clemente Island (SCI), owned and operated by the U.S. Navy since 1934, is an example of a disturbed open shrubland community in need of a high-quality, consistent vegetation map to support ecological management and rehabilitation efforts. Systematic mapping of SCI's vegetation was initially undertaken in 1980 (Sward & Cohen, 1980), and a revised map was produced in 2011 (Tierra Data Inc., 2013). While the latter mapping effort provided an update of the 1980 map, Navy resource management personnel determined that greater spatial detail and improved classification and mapping were required to best support management of natural resources at SCI.

The primary objective of this study is to map the distribution and quantify the cover of vegetation alliances over the entirety of SCI. As part of this objective, we develop and evaluate mapping methods specific to open-canopy shrublands.

2 | METHODS

2.1 | Study area

The study area is San Clemente Island, the southernmost and fourth largest (145 km²) of the eight Channel Islands located off the coast of southern California. The island lies about 102 km westnorthwest of San Diego (Figure 1). Precipitation timing follows a typical Mediterranean climate pattern of warm, dry summers and cool, wet winters. Average annual precipitation across the island is 20 cm, with values ranging from 14.2 to 23.1 cm (Tierra Data Inc., 2011; Hiebert, Durzi, Garstka, & Zink, 2017). The terrain of the island is varied, with the western portion characterized by marine terraces, the interior of the island by a broad plateau reaching close to 600 m in elevation, and the eastern portion of the island by a high coastal escarpment that is dissected by steep canyons.

Vegetation patterns on SCI have been strongly modified by heavy grazing pressure from exotic herbivores. Sheep, goats, cattle, and mule deer have all been present at some point on the island (Schoenherr, Feldmeth, & Emerson, 2003). Sheep and cattle ranching ended in 1934, mule deer died around the 1970s, and pigs and goats were removed by the early 1990s (Keegan, Coblenz, & Winchell, 1994; Schoenherr et al., 2003). Prolonged grazing pressure substantially altered the vegetation, with some species persisting only on inaccessible steep cliffs (Raven, 1963). Following removal of grazing pressure, shrub recovery

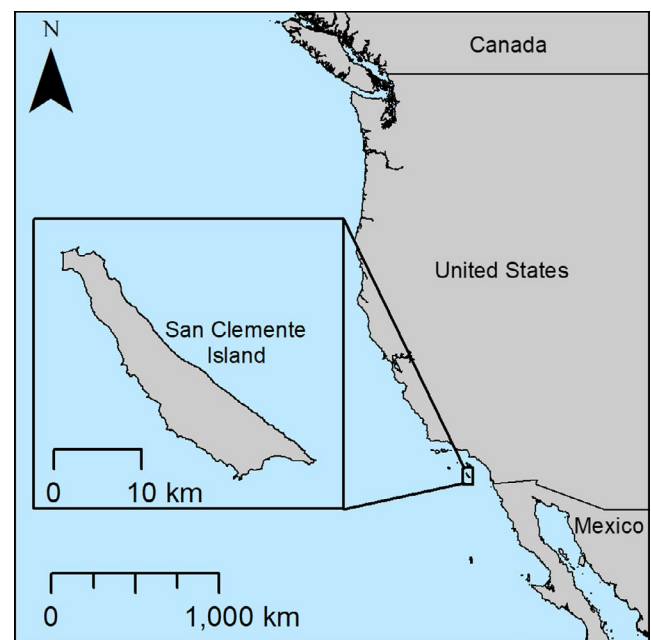


FIGURE 1 Map of San Clemente Island study area [Colour figure can be viewed at wileyonlinelibrary.com]

has been observed, most notably for *Artemisia californica*, *Rhus integrifolia*, *Heteromeles arbutifolia*, and *Baccharis pilularis* (Tierra Data Inc., 2011). Plant nomenclature follows Baldwin et al. (2012). While global patterns of shrub encroachment are commonly associated with habitat degradation (Eldridge et al., 2011), at SCI the recovery of these native shrub species is viewed as a positive sign of increasing ecosystem health (Tierra Data Inc., 2011).

The most abundant native vegetation is maritime cactus scrub characterized by dominance of either *Opuntia littoralis*, *Lycium californicum*, or *Cylindropuntia prolifera*. *Lycium californicum*-dominated areas are found along the west coast, *Opuntia littoralis* dominates just inland from the *Lycium californicum* areas, and *Cylindropuntia prolifera* is common in the southern portion of the island. Native and non-native grasses are common in the interior of the island (Junak et al., 2007). Coastal sage scrub dominated by *Artemisia californica* is common along the eastern escarpment, and maritime chaparral dominated by *Rhus integrifolia* is present within canyons. Also present within canyons are the broadleaf woodlands, dominated by *Prunus ilicifolia* ssp. *lyonii*, *Quercus tomentella*, or *Lyonothamnus floribundus* ssp. *aspleniifolius*. *Baccharis pilularis* is dominant on the upper plateaus. SCI is home to nine threatened or endangered species, which are managed by the Navy (Tierra Data Inc., 2013). Populations have benefited from the removal of non-native herbivores from the island; however, they still face threats from habitat degradation, competition from non-native plant species, erosion and increased fire frequency (Tierra Data Inc., 2013).

2.2 | Classification system

We designed the vegetation community and land cover classification system implemented for this mapping project to follow the Manual of California Vegetation (MCV) (Sawyer et al., 2009) classification system, which is compatible with U.S. National Vegetation Classification standards. The MCV classification system represents a needed effort to establish a consistent and defensible vegetation classification system to be used by local, state, and federal resource agencies in California. In order to maintain consistency with current implementations of the MCV system, we used an existing field-based classification key developed for western San Diego County (Sproul et al., 2011) as the starting point for our classification key. This key consists of a set of mapping rules which specify species composition requirements and cover thresholds, and the order in which vegetation communities should be assessed to delineate vegetation polygons and assign an appropriate category label. We made adjustments to the key based on evaluation of field data from the San Clemente Island Land Condition and Trend Analysis data set (Tierra Data Inc, 2011), meetings with the end users of the mapping product, and preliminary field observations. The smallest size areal unit delineated on the map, or minimum mapping unit (MMU), varied by category. For most categories, an MMU of 0.25 hectares (ha) was used, but areas of special interest were mapped with finer MMUs, as shown in Appendix S1.

Eight of the 19 map classes defined for this study represent vegetation alliances, which are floristically defined by MCV as vegetation types identified by their dominant or characteristic species (Sawyer et al., 2009). Two classes represent associations, which are finer floristic units within alliances. Other map classes include vegetation groups, stands, and land cover types organized within the MCV hierarchical classification structure (Appendix S1). Collectively we refer to these as “vegetation communities.” We followed the California Native Plant Society (CNPS) rapid assessment and relevé protocols to collect plot level data for delineated vegetation communities from summer 2016 through spring 2017. Both the rapid assessment and relevé methods call for recording site information and percent cover by species in stands defined by consistent species composition and structure. In relevés, all species present within a bounded area (typically 10 m × 10 m for herbaceous stands or 20 m × 20 m for shrubland stands) are recorded. In rapid assessment plots, the first 20 species with the highest cover are recorded within a representative portion of the stand.

We stratified plots by vegetation type and conducted 38 rapid assessment and 16 relevé plots for 13 of the vegetation classes. The full mapping key developed for this project is available in Appendix S2.

2.3 | Data

A commercial aerial survey company captured digital imagery in November 2015 to yield a four-band, digital multispectral image data set, having a very high spatial resolution of 0.15 m. Imagery was acquired with a dual camera imaging system, consisting of two Canon Mark II 5D Digital SLR cameras (21 megapixel), with one camera capturing imagery in the visible spectrum and one modified to capture near-infrared (NIR) imagery. The sensor system was operated on a Cessna 182 fixed-wing aircraft, and approximately 8,000 individual images were captured with each camera for coverage of the entire island. These image frames were collected with approximately 80% forward and sideward overlap. This very high spatial resolution (VHSR) ortho-imagery was the primary source of imagery for the vegetation mapping project.

We generated a Digital Surface Model (DSM) based on Structure from Motion technology using Agisoft Photoscan software—Agisoft LLC, St. Petersburg, Russia. Photoscan software and the DSM were utilized to georeference, orthorectify, and mosaic imagery to create a seamless orthoimage mosaic of the island projected in the WGS 1984, UTM Zone 11N coordinate system. National Agriculture Imagery Program (NAIP) imagery collected in 2016 was used as a reference source to place 18 ground control points, and root mean squared error for the registration was 4.23 m. The resulting level of registration would have been appropriate for many mapping projects, but we noticed in early testing that in some areas, the locations of individual shrubs were offset between the VHSR imagery and the lidar data set by the diameter of an entire shrub. The 2016 NAIP showed very close agreement with the lidar, so we used it as a reference source to further refine the registration using AutoSync

Workstation in ERDAS Imagine—Hexagon Geospatial, Madison, AL, USA.

NAIP imagery captured in 2012, 2014, and 2016 was also used as input for image classification. These ortho-images are four-band (R, G, B, NIR) data sets, but have a coarser spatial resolution of 0.6 m in 2016 and 1 m in 2014 and 2012. These products were mostly used when portions of the higher spatial resolution imagery contained dark shadow pixels. A summary of all raster data sets utilized is given in Appendix S3.

Several vector map products were also utilized for image classification (Appendix S4). Records of San Clemente loggerhead shrike (*Lanius ludovicianus mearnsi*) nesting sites (with species of nesting substrate) were used during the accuracy assessment phase.

We used other data sets as calibration for rule set development as listed in Appendix S5. These included a vegetation map generated to assess San Clemente Island Bell's sparrow (*Amphispiza belli clementeae*) habitat (Meiman et al., 2017), Land Condition and Trend Analysis plots monitored from 1992 to 2010, and a set of over 400 geotagged photos collected during our field work.

We used previously collected lidar data to create a model of vegetation canopy height, also known as a normalized Digital Surface Model (nDSM), as detailed in Appendix S6. Full waveform lidar data were collected in fall 2014 (Chadwick et al., 2016; Melville et al., 2016). The reported vertical accuracy is 10 cm.

2.4 | Imaging analysis

Once the classification system was established, mapping procedures based on a hierarchical object-based image analysis (OBIA) approach were developed, tested, and implemented, followed by manual editing and then an accuracy assessment of the final product. The overall workflow is illustrated in Figure 2. Our emphasis was on establishing a reliable, semi-automatic image classification approach that minimized the need for more subjective and work-intensive manual mapping and editing. This required substantial research and development activities.

2.4.1 | Object-based image analysis approach

We employed a hierarchical object-based classification based on a rule-based expert system and implemented it with eCognition software—Trimble Inc., Sunnyvale, CA, USA. Rather than classifying individual pixels, an OBIA approach first groups spatially contiguous pixels into segments, or “objects,” and conducts classification on the object level. Numerous studies have shown superior mapping results with an OBIA approach compared to a pixel-based approach to image classification based on high spatial resolution image data (Blaschke et al., 2014). An OBIA approach has been shown to be effective for both life-form mapping (Laliberte et al., 2004; Hamada, Stow, & Roberts, 2011; Freeman, Stow, & Roberts, 2016) and

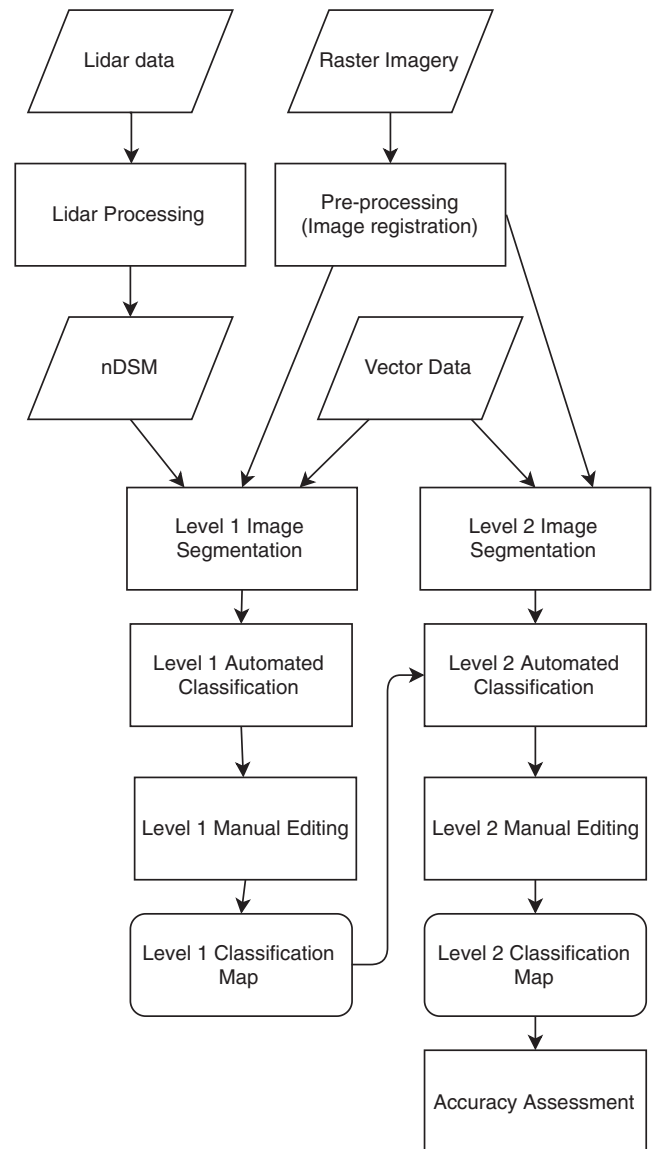


FIGURE 2 Flowchart for image-based vegetation mapping procedures

species-level mapping (Uyeda, Stow, O'Leary, Schmidt, & Riggan, 2016) in southern California shrublands and forests. While the use of OBIA is well established, our study is one of the first to use OBIA for vegetation community mapping based on enforcement of percent cover thresholds. We used eCognition Developer version 9 for research and development, and the eCognition Server for island-wide data processing.

One of the strengths of eCognition is the ability to use multiple levels for hierarchical segmentation and classification. Image segments at the lower level (i.e., finer scale or Level 1) are nested within higher level (i.e., coarser scale or Level 2) segments (Figure 3). For Level 1, the resultant objects (i.e., classified segments) are the same size or smaller than individual shrubs or small patches of a homogeneous land cover type. For Level 2, objects represent vegetation and land cover patches and stands. We classified Level 1 objects to at least the growth-form level (or land cover type for

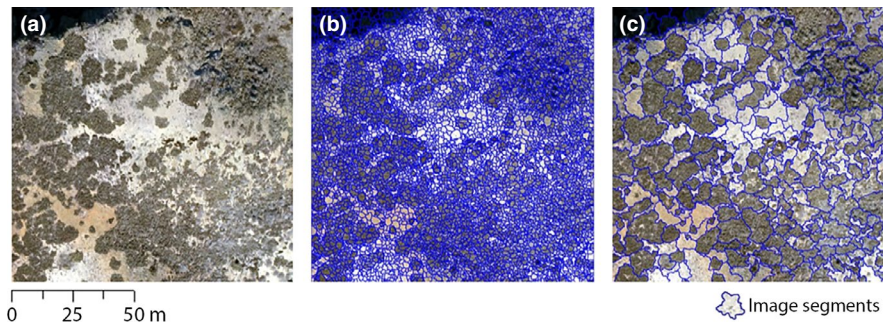


FIGURE 3 Example of: (a) RGB image, (b) image segments produced at Level 1, and (c) image segments produced at Level 2 [Colour figure can be viewed at wileyonlinelibrary.com]

non-vegetated areas), and to species level for shrubs and trees. We then used the percent cover of species present within the Level 2 objects to identify the community type, the key advantage of this hierarchical approach. This process of first determining the mix of species present within a Level 2 object, then calculating the percent cover of each species, and finally applying a mapping rule set to make the final community type determination is similar to how human interpreters make decisions when mapping in the field. Although the semi-automated image-based approach often entails greater uncertainty about whether a given species has been correctly mapped, such an approach is much more reliable and consistent at quantifying percent cover of alliance-defining species.

2.4.2 | Level 1 segmentation, classification and generalization/refinement

Level 1 categories correspond to the species that define the vegetation community types shown in Appendix S1, with additional classes for shrubs and trees that could not be identified at the species level. A shadow class was also used to identify portions of steep canyons that were in shadow at the time of imagery acquisition, providing a basis for image stratification and separate classification of shadow and non-shadow areas. Approximately 5% of the total area was initially classified as this shadow class. Salt marsh alliances have such limited distributions that we manually digitized these classes based on image interpretation, ground-based photos, and a historic wetland delineation report (Bitterroot, 2002).

We used the eCognition multiresolution segmentation algorithm with a scale parameter of 10, a shape weight of 0.5, and compactness weight of 0.7. These parameters were deemed optimal through interactive testing and visual assessment. The raster inputs for the Level-1 segmentation include the four-band (R, G, B, NIR) VHSR imagery and the nDSM (canopy height) layer. The segmentation algorithm starts with a single pixel and uses the values provided in the raster inputs to merge the pixel with neighbors based on spectral-radiometric homogeneity criteria. The final size of the segments generated is related to the magnitude of the scale parameter, although the parameter does not directly define an object size. We also included two vector layers as inputs in the segmentation algorithm: developed areas and coastline extent. These vector layers did not

influence the size or composition of segments, but ensured that the objects generated did not cross the boundaries defined by the vector layers.

Image segments were classified using a rule-based expert system. Trained image interpreters created rule sets to assign a class to each segment based on spectral, height, and contextual information. The algorithms used in the rule set are provided in Appendix S7, and the object features are provided in Appendix S8. In addition to the VHSR ortho-imagery and nDSM layer, we included four-band NAIP ortho-images and normalized difference vegetation index (NDVI) images generated from them. NDVI images depict spatial distributions of the amount and condition of above ground green vegetation and are calculated by subtracting the digital number values of the red band from the NIR band and dividing by the sum of the NIR and red band values (Jensen, 2007). NDVI calculated from the VHSR is also included as input in the classification. A sub-hierarchy was utilized within the Level 1 objects, as we first classified objects into general categories of shadow/non-shadow, and then non-shadow objects were classified as vegetation/non-vegetation. Objects in the vegetation category were further classified into tree, shrub, and herbaceous categories, then eventually into the species-specific classes. Non-vegetation objects were assigned to “Developed” (defined entirely by the bounds of the developed area vector layer) or “Bare” (based on spectral, height, and contextual information) classes. Shadowed segments were eventually classified as a vegetation or land cover class based on modified thresholds and/or thresholds calculated from non-shadowed segments.

We used an iterative process to create rule sets for each Level 1 class, first testing possible approaches on a small area, extending it to a larger area, then modifying the approach as necessary to improve results. We delineated 15 regions across the island (shown in Figure 4) in which tailored rule sets were developed. We started by implementing the same base rule set for all regions, then we identified areas with poor classification results in each region and adjusted the rule set for only that region to improve the results. This approach helped avoid classification errors caused by broad application of a single rule set, where rule adjustments that improve the classification in one area result in poor classification elsewhere.

The segmentation of Level 1 objects is very computationally intensive, and attempting to produce segments with a small-scale

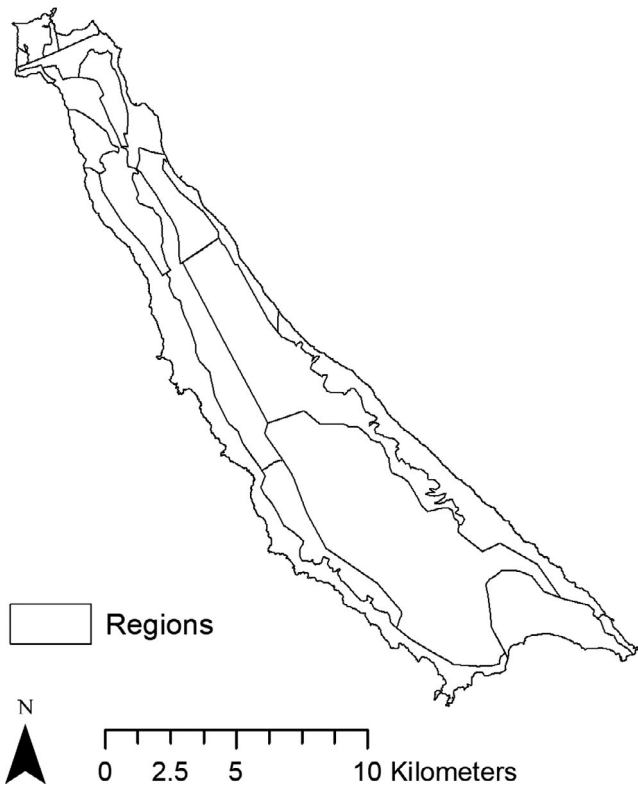


FIGURE 4 Fifteen regions delineated based on homogenous vegetation and terrain characteristics, to enable efficient and more accurate image classification

parameter over a large area frequently caused the software to fail. To address this issue, we generated overlapping tiles of classification products that were mosaiced together along their centerlines (O'Neil-Dunne, MacFaden, Royar, & Pelletier, 2013). We divided all raster inputs into 29 tiles that covered the extent of the island with 10% overlap and performed batch processing using two eCognition Server licenses. We then conducted manual editing of the semi-automated Level 1 product using tools within eCognition.

2.4.3 | Level 2 segmentation and classification

As in the Level 1 segmentation, we used the multiresolution segmentation algorithm with a shape weight of 0.5 and compactness weight of 0.7 for Level 2, though a larger scale parameter of 100 was deemed appropriate in generating larger segments that were closer to the size of the final community-type polygons. Only the 2015 VHRS imagery was included as a raster input for segmentation. The developed and coastline vector layers were included to avoid generating objects that crossed these boundaries. The hierarchical structure of levels within eCognition ensured that Level 1 objects were completely contained by constraining the Level 2 segmentation.

The Level 2 mapping rules are defined by both absolute cover of a particular growth form (herb, shrub, or tree) and the relative cover

of the diagnostic species within a growth form. We used the "Relative area of" function within eCognition to calculate the percent cover of each shrub species and relative cover where necessary for the field-based mapping key, then implemented the rules in the key to assign the correct community type for each Level 2 object. In order to ensure that adjacent but unconnected objects of a given community type were properly grouped, we used the pixel-based object resizing algorithm within eCognition to expand a given community type object to annex unclassified objects. We then merged unclassified objects with appropriate neighboring objects until all objects met the MMU thresholds.

2.4.4 | Level 2 generalization and manual editing

To improve the cartographic appearance of and generalize the final map product, we applied a smoothing algorithm to the polygons of the Level 2 community type map. Both Level 1 and 2 products were exported from eCognition as overlapping tiled rasters, then mosaiced to yield a single raster file using the mosaic tools in ERDAS Imagine. By mosaicing the overlapping tiles along the middle of the seamlines, edge effects were reduced. The Level 2 product was converted to a vector file. At this stage a team of two map analysts visually examined and interactively refined the map, fixing straight lines artifacts resulting from the seamline mosaicing procedure, editing misclassified or poorly delineated Level 2 polygons, and performing a topology check.

2.4.5 | Overall map accuracy assessment

Due to the large spatial extent and access restrictions associated with conducting field work on SCI, we conducted an accuracy assessment primarily using an independent ultra-high spatial resolution (UHSR) aerial imagery data set with even finer spatial resolution (4–6 cm) than the 2015 VHRS imagery (Appendix S3). Images were captured intermittently along a series of eight flight lines in August 2017 with the same aircraft and imaging system (Figure 5). A total of 311 image frames were collected, with an average areal coverage of 9 ha. Each frame was independently georeferenced. Three circular polygons, each with an area of 0.25 ha, were randomly located in each frame. These three circular areas per frame served as potential units for assessing accuracy. An independent image interpreter (not involved in rule set development) was trained to identify the species/land cover classes in Appendix S1 on either true color or color infrared displays of the 2017 UHSR imagery. For the first two circular units in each frame, the image interpreter visually estimated the percent cover of the three classes having the greatest proportional cover. These values were recorded and used to determine the appropriate community type using the mapping key in Appendix S2. The image interpreter also recorded whether the site associated with the circular unit had burned (defined by the presence of at least 5% cover of ash or charred material) and a subjectively measured level of confidence in the class assessment (low, medium, or high confidence). The third circular assessment unit per frame was only assessed in cases where one of the first two polygons

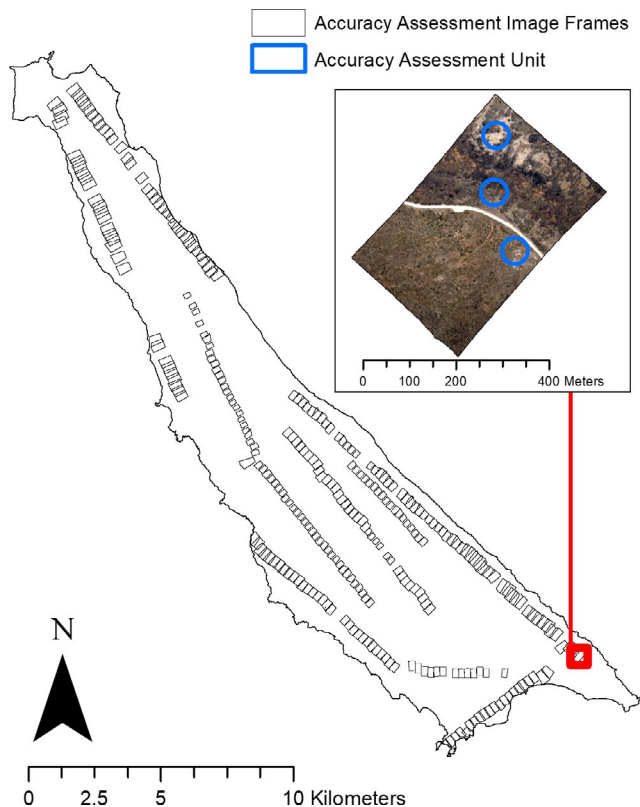


FIGURE 5 Flight lines and image frames for the 2017 UHSR accuracy assessment data set. Inset depicts an ultra-high spatial resolution aerial image displayed as RGB, with three circular accuracy assessment units randomly placed [Colour figure can be viewed at wileyonlinelibrary.com]

contained a recently severely burned patch, or where there was a clear mixture of community types within the polygon. A total of 46 assessment units that were deemed low confidence during image interpretation were visited in the field to aid in community type assignment for reference data generation.

Since the accuracy assessment units were selected randomly and independent of the mapping effort, they sometimes spanned more than one polygon in the community-level map. It was necessary to determine which class covered the largest portion of the sampling unit. However, for classes with low thresholds for cover in the original mapping key, it was sometimes most appropriate to consider a class with less than majority cover as representative of the mapped class for a given polygon. For example, a given accuracy assessment polygon might cover an area mapped as 60% California Annual and Perennial Grassland Macrogroup and 40% *Baccharis pilularis* Alliance. If the image interpreter performing the accuracy assessment noted the cover of just 5% *Baccharis pilularis* in that assessment polygon, the mapping rules would require it to be classified as *Baccharis pilularis* Alliance (see mapping key in Appendix S2). Although the majority class in this case is California Annual and Perennial Grassland Macrogroup, it is not the class the image interpreter would have selected when viewing the assessment polygon. Class assignments were therefore made by selecting the first community type that met the following criteria: (a)

if woodland trees were present, at least 5% cover would classify the entire polygon as that tree alliance; (b) if shrubs were present, the assigned shrub class was that having at least 30% cover of the polygon and was also the majority shrub class; (c) developed land cover needed to occupy at least 50% of the circular unit to classify it as Developed; and (d) herbaceous community types were determined by the majority community type. It was not possible to use the exact same values for the shrubs as was used in the mapping key, as percent cover of a class in the community-level map is not the same as percent cover at the scale of individual shrubs in an open-canopy shrubland. Since trees were mapped at the level of individual canopies, it was possible to use the same 5% threshold for the class assignment. Selecting only accuracy assessment units that were located entirely within a single mapped class would eliminate the need for the set of thresholds described above, but would bias the assessment toward more homogeneous areas, and would not fully capture the accuracy of areas of transition between two or more classes.

We calculated accuracy using both a traditional and fuzzy accuracy assessment scoring procedure. While a traditional accuracy assessment comparison is binary (correct/incorrect), a fuzzy accuracy assessment comparison gives a score that reflects the degree to which an incorrect class was partially correct. For the fuzzy assessment, we used a system with scores from 0 to 5 based on CNPS procedures (Stout, Buck-Diaz, Taylor, & Evens, 2013), as shown in Table 1. We compared the number of accuracy assessment units that exactly matched the mapping category to those with a score equal to or greater than 3 (Woodcock & Gopal, 2000).

2.4.6 | Tree/chaparral accuracy assessment

Although the 2017 UHSR imagery collected to generate reference data for the overall map accuracy assessment provided some coverage of the canyon woodlands and maritime chaparral, coverage was not adequate given the small MMU used and limited occurrence of these alliances. For the tree/chaparral classes, we used coded and georeferenced observations of nesting substrate (plant species or vegetation

TABLE 1 Scoring system used for fuzzy accuracy assessment

Score	Description
0	Completely wrong growth form (e.g., shrub, tree, or herb-grass), minimal ecological similarity
1	Same growth form
2	Match at three levels up from lowest level classified, usually Division
3	Match at two levels up from lowest level classified, usually Macrogroup
4	Match at one level up from lowest level classified, usually Group, or overlap in diagnostic species
5	Perfect match

class) from the San Clemente loggerhead shrike nesting surveys, which had not been used as input for the initial mapping effort.

A total of 77 trees in the shrike habitat data set were used to determine the accuracy in tree/chaparral shrub identification. The species recorded include *Rhus integrifolia*, *Prunus ilicifolia* ssp. *lyonii*, *Lyonothamnus floribundus* ssp. *aspleniifolius*, and *Quercus tomentella*. We tested both species-level accuracy and pooled tree/chaparral shrub accuracy (allowing for confusion of *Rhus integrifolia*, *Prunus ilicifolia* ssp. *lyonii*, *Lyonothamnus floribundus* ssp. *aspleniifolius*, and *Quercus omentella* as long as a tree or chaparral shrub was detected). Such an approach to accuracy assessment does not reveal whether trees are over-mapped.

3 | RESULTS

3.1 | Vegetation community map product

The final vegetation map portrays the distribution of 19 vegetation community types across SCI (Figure 6). An interactive web map can be found at <https://arcg.is/1HzTa1>. The *Lycium californicum* Alliance is most abundant along the western coast, with increasing *Opuntia littoralis* Association just inland from the *Lycium californicum* areas. The *Artemisia californica* Alliance is common along the eastern coast. Much of the interior of the island is covered in Annual and Perennial Grassland.

The coverage of each community type by area and associated statistics are given in Appendix S9. The most abundant community or land cover type is the California Annual and Perennial Grassland Macrogroup, which covers over 35% of the island. The *Opuntia littoralis* Association is the next most abundant type, with 27% coverage. These two communities, combined with the *Lycium californicum* Alliance and *Artemisia californica* Alliance, cover almost 90% of the island. *Rhus integrifolia* individuals were most abundant in terms of number of discrete polygons ($n = 13,063$), followed by *Prunus ilicifolia* ssp. *lyonii* individuals ($n = 1,620$) and *Lyonothamnus floribundus* ssp. *aspleniifolius* individuals (1,516), although the high numbers of these tree and chaparral species is mostly due to the very fine MMU at which they were mapped.

3.2 | Overall map accuracy assessment

A total of 531 accuracy assessment polygons were assessed. More than a third (a total of 186) of those polygons showed some evidence of a recent burn. The overall map accuracy from the fuzzy accuracy assessment is 79%, with many polygons receiving a partial score due to a high degree of overlap in diagnostic species (Appendix S10). The traditional accuracy assessment of all polygons produced an overall accuracy of 61%, as shown in Table 2. A total of 13 of the 19 mapping classes were identified in the reference data, with rare classes often being underrepresented. The classes included in the assessment make up 98% of the total area of the island (Appendix S9). Including

only high confidence polygons yielded an accuracy estimate of 70% ($n = 125$, Appendix S11). Including only the polygons that contain a single community type produced an accuracy rate of 77% ($n = 226$, Appendix S12).

The *Ambrosia chamissonis*–*Abronia maritima* Alliance was mapped most accurately across the island, with 92% producer's accuracy and 100% user's accuracy for 11 accuracy assessment units (Table 2). The California Annual and Perennial Grassland Macrogroup was also mapped fairly successfully, with 82% producer's accuracy and 60% user's accuracy. Confusion between grasslands and the *Opuntia littoralis* Association was the main reason for the higher error in the user's accuracy calculation for this macrogroup. The *Opuntia littoralis* Association, *Lycium californicum* Alliance, and *Artemisia californica* Alliance were frequently confused with one another, possibly due to the similar height of key shrub species and co-occurrence of the same or similar plant species, especially non-native grasses. The accuracy of the canyon woodlands is low, although these alliances are better evaluated in the separate tree/chaparral shrub accuracy assessment (Tables 2 and 3).

3.3 | Tree/chaparral accuracy assessment

The rate of successful tree identification is 81%, but species-level identification accuracy is 45% (Table 3). The highest producer's accuracy was found for *Quercus tomentella* at 86% (6 out of 7 individuals recorded in the shrike habitat data set were correctly identified in the Level 2 map). *Prunus ilicifolia* ssp. *lyonii*, *Rhus integrifolia*, and *Lyonothamnus floribundus* ssp. *aspleniifolius* were frequently confused with each other, and *Prunus ilicifolia* ssp. *lyonii* and *Rhus integrifolia* were sometimes confused with *Artemisia californica*.

4 | DISCUSSION

4.1 | Vegetation community distribution

The category with the greatest extent of coverage on the island is California Annual and Perennial Grassland. While this category combines native perennial grasses and non-native annual grasses, the majority of the cover is comprised of non-native grasses. We might expect coverage of this category to be shrinking as shrubs continue to expand into their historic range following the release of grazing pressure as observed from long-term monitoring (Tierra Data Inc., 2011). At the same time, the cover of annual grasses within shrubland and other vegetation communities has been observed to be higher in the period after release from grazing pressure (Wylie, 2012). A study of long-term transects at SCI showed an increase in non-native grass cover after the removal of non-native herbivores, but with only one year of sampling conducted after grazing cessation, it is not possible to completely separate

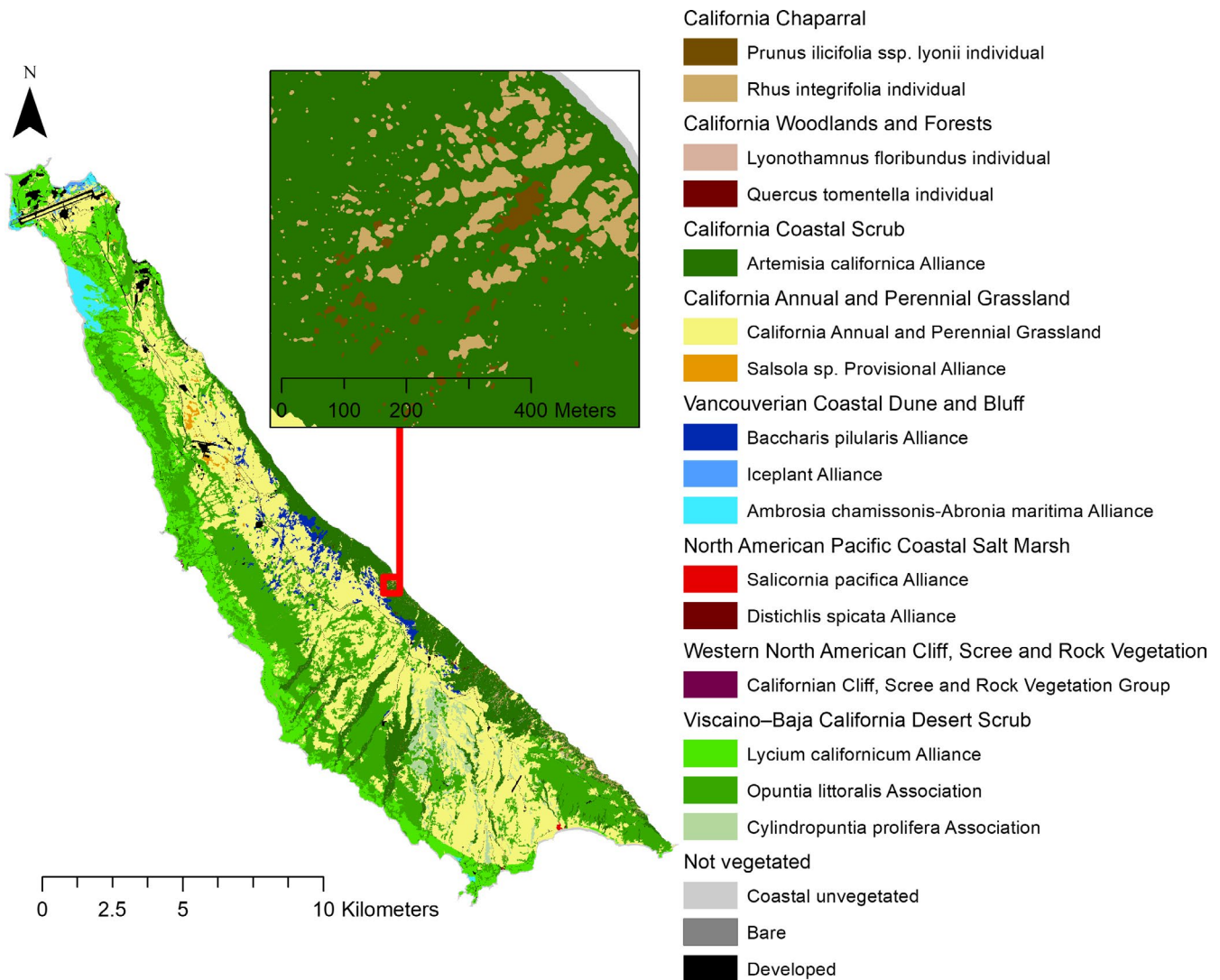


FIGURE 6 Final vegetation mapping results, with vegetation communities organized by Macrogroup. An interactive web map can be found at <https://arcg.is/1WuC1K> [Colour figure can be viewed at [wileyonlinelibrary.com](https://onlinelibrary.wiley.com)]

the effect of interannual variation in precipitation (Wylie, 2012). Low soil moisture is associated with low cover of non-native plants on SCI, so drought conditions likely play a role in limiting the cover of non-native grasses (Paudel et al., 2017). It is difficult to show clear patterns of change from historic maps due to differences in the mapping approaches, minimum mapping unit, and classification systems. Future vegetation community mapping using the same classification scheme and techniques applied here should be used to monitor changing grassland patterns at SCI and elsewhere, as well as provide a basis for investigating the influence of some of these drivers. Although a new effort would require calibrating the rule set to a new imagery set, the structure of the rule set and image analysis process tree, as well as greater repeatability of the semi-automated approach will facilitate more consistent future mapping compared to manual aerial image interpretation or field mapping approaches.

The abundance of the *Opuntia littoralis* Association, *Lycium californicum* Alliance and *Artemisia californica* Alliance (comprising 53%

combined cover) is an encouraging sign for the island. These vegetation types are important habitat for the San Clemente Island Bell's sparrow and San Clemente loggerhead shrike, both of which are island endemics and federally listed under the Endangered Species Act (Tierra Data Inc., 2013). Nesting habitat for the San Clemente loggerhead shrike also occurs within *Prunus ilicifolia* ssp. *lyonii*, *Rhus integrifolia*, *Artemisia californica*, and *Baccharis pilularis* shrubs (Stahl, Gunther, Desnoyers, Bridges, & Garcelon, 2011). Improvements in differentiating these three types (discussed below) could support more refined habitat preference studies and type-specific monitoring and management.

The vegetation community types mapped as part of this project reflect the management priorities of the map users. This results in a map with a high emphasis on the recently recovering tree and chaparral shrub species. A counterintuitive result of using a small MMU is that the map might reflect a smaller total area for trees and chaparral than a mapping effort with a larger MMU, because only the delineated canopies of the trees will be mapped, with adjacent

TABLE 2 Overall accuracy assessment error matrix

	Reference data															Row total	User's accuracy (%)
	<i>Ambrosia chamissonis</i> ...	<i>Artemisia californica</i> ...	<i>Baccharis pilularis</i> ...	Bare	California... Grassland	<i>Cylindropuntia prolifera</i> ...	Developed	<i>Lycium californicum</i> ...	<i>Lyonothamnus</i> ...	<i>Mesembryanthemum</i> ...	<i>Opuntia littoralis</i> ...	<i>Prunus ilicifolia</i> ...	<i>Quercus tomentella</i> ...	<i>Rhus integrifolia</i> ...	<i>Salsola</i> sp. Provisional...		
<i>Ambrosia chamissonis</i> ...	11	0	0	0	0	0	0	0	0	0	0	0	0	0	0	11	100
<i>Artemisia californica</i> ...	0	36	4	1	2	1	0	2	1	0	25	0	4	2	0	78	46
<i>Baccharis pilularis</i> ...	0	3	9	0	2	0	0	0	0	0	1	0	0	0	0	15	60
Bare	0	0	0	0	0	0	0	0	0	0	0	0	0	0	0	0	0
California... Grassland	0	5	3	5	93	5	0	2	0	5	36	0	0	0	0	154	60
<i>Cylindropuntia prolifera</i> ...	0	0	0	0	1	1	0	0	0	0	5	0	0	0	0	7	14
Developed	0	0	0	1	0	0	6	0	0	0	0	0	0	0	0	7	86
<i>Lycium californicum</i> ...	0	2	0	1	4	2	1	26	0	0	7	0	0	0	0	43	60
<i>Lyonothamnus floribundus</i> ...	0	1	0	0	0	0	0	0	0	0	0	5	0	0	0	6	0
<i>Mesembryanthemum s...</i>	0	0	0	0	0	0	0	0	0	1	0	0	0	0	0	1	100
<i>Opuntia littoralis</i> ...	0	6	2	0	9	9	0	19	0	0	127	0	0	1	0	173	73
<i>Prunus ilicifolia</i> ...	0	0	0	0	0	0	0	0	1	0	1	0	2	0	0	4	0
<i>Quercus tomentella</i> ...	0	0	0	0	0	0	0	0	0	0	0	0	4	0	0	4	100
<i>Rhus integrifolia</i> ...	1	0	0	0	1	0	0	1	0	0	3	0	8	10	0	24	42
<i>Salsola</i> sp. Provisional...	0	0	1	0	2	1	0	0	0	0	0	0	0	0	0	4	0
Column total	12	53	19	8	114	19	7	50	2	6	205	0	23	13	0	531	
Producer's accuracy (%)	92	68	47	0	82	5	86	52	0	17	62	0	17	77	0		
Total accuracy: 61%																	

^aThe values on the diagonal show the number of polygons for each class that are in agreement in both the map and reference data source.

shrubs and grasslands not included in the total area. Alternatively, if shrub and tree patches are omitted entirely due to a larger MMU, the presence of small patches of vegetation will not be recorded at all, as documented by Stohlgren, Chong, Kalkhan, and Schell (1997). For correct interpretation, it is important to select an appropriate MMU size when comparing vegetation cover types or maps from different years or regions.

4.2 | Lessons learned regarding semi-automated OBIA approach

The mapping strategy of hierarchical object-based classification with a rule-based expert system is a valuable approach that yielded a useful vegetation community map product. This approach is particularly advantageous in open-canopy systems, which are not neatly defined by a continuous pattern of shrubs or trees, but are instead patchily distributed. Human interpretation of vegetation pattern in the field and from imagery can vary greatly in both spatial positioning and

classification choice (Ullerud, Bryn, Halvorsen, & Hemsing, 2018), so the use of a semi-automated, rule-based system helps greatly to standardize the mapping procedure. However, the effort involved in percent cover calculations might provide less utility in areas with higher shrub and tree cover (Dobrowski, Safford, Cheng, & Ustin, 2008).

Percent cover rules for both relative and absolute cover were readily implemented in eCognition. Determining the appropriate scale parameter for image segmentation involved some trial and error. A small-scale parameter created segments too small to contain the heterogeneous shrub cover upon which the percent cover rules were based; whereas many segments produced from a large-scale parameter encompassed multiple community units. The ability to include context (for example, classifying segments partially based on the proximity to members of a given community type) greatly improved the classification results. The inclusion of the nDSM greatly enhanced the classification accuracy in shrub-dominated areas, as detailed in Snaveley, Uyeda, Stow, O'Leary, and Lambert (2019).

TABLE 3 Error matrix of species-level tree/chaparral shrub observations. Tree/chaparral shrub accuracy is a measure of agreement for pooled tree/chaparral species (*Lyonothamnus floribundus*, *Prunus ilicifolia*, *Quercus tomentella*, *Rhus integrifolia*)

	Reference data								Row total	User's accuracy
	<i>Artemisia californica</i> Alliance	California Annual and Perennial Grassland	<i>Cylindropuntia prolifera</i> Association	<i>Lyonothamnus floribundus</i> ssp. <i>asplenifolius</i> individual	<i>Opuntia littoralis</i> Association	<i>Prunus ilicifolia</i> ssp. <i>lyonii</i> individual	<i>Quercus tomentella</i> individual	<i>Rhus integrifolia</i> individual		
<i>Artemisia californica</i> Alliance	0	0	0	0	0	3	0	7	10	0
California Annual and Perennial Grassland	0	0	0	0	0	0	0	1	1	0
<i>Cylindropuntia prolifera</i> Association	0	0	0	0	0	1	0	1	2	0
<i>Lyonothamnus floribundus</i> ssp. <i>asplenifolius</i> individual	0	0	0	3	0	5	0	2	10	30
<i>Opuntia littoralis</i> Association	0	0	0	0	0	0	0	1	1	0
<i>Prunus ilicifolia</i> ssp. <i>lyonii</i> individual	0	0	0	2	0	9	1	7	19	47
<i>Quercus tomentella</i> individual	0	0	0	3	0	0	6	0	9	67
<i>Rhus integrifolia</i> individual	0	0	0	1	0	7	0	17	25	68
Column total	0	0	0	9	0	25	7	36	77	
Producer's Accuracy	0	0	0	33	0	36	86	47		

Total accuracy: 45%

Tree/chaparral shrub accuracy: 81%

^aThe values on the diagonal show the number of polygons for each class that are in agreement in both the map and reference data source.

While the UHSR imagery collected in 2017 allowed for efficient accuracy assessment, 2017 was a particularly severe fire year (Hiebert et al., 2017). Many assessment areas burned after the mapping imagery was collected in 2015, confounding efforts to identify the original community type.

4.3 | Limitations

A major issue we encountered during image processing was error in co-registration between the VHSR imagery, NAIP imagery, and lidar data set. Although we refined the co-registration accuracy of the various ortho-images and the nDSM layer, we were not able to match the imagery suitably for all areas, especially for steep canyons. Small registration errors may not be a problem for areas with large trees. However, a few decimeters of offset in a small shrub canopy can mean that the information contained in the image layer is completely offset from the canopy height information in the nDSM.

While our vegetation mapping approach is mostly successful in detecting the presence of trees and chaparral shrubs, identifying these individuals to the species level is problematic due to similar spectral signatures within the broad-band visible and near-infrared imagery, and the location of these trees in deep canyons with low illumination. While the dominant shrubs on the island (*Opuntia littoralis*, *Lycium californicum*, and *Artemisia californica*) each have unique

spectral signatures and contextual properties, those associated with the trees on the island are more similar, making tree species much more difficult to distinguish.

The accuracy assessment approach used for this study was based on a large number of plots without being constrained by whether a plot was accessible in the field, but did result in rare classes being undersampled. We were able to accommodate this undersampling issue for trees and shrubs by incorporating a second assessment focused on species of these growth forms, but were not able to adequately sample some of the less abundant classes. Several of these rare classes were included in the classification scheme because of their importance for management (e.g. *Salsola* sp. Provisional Alliance, *Distichlis spicata* Alliance, Californian Cliff, Scree and Rock Vegetation Group, *Salicornia pacifica* Alliance). The Coastal Unvegetated class was included to enable full coverage of the island. The beaches and rocky shoreline forming this class were not the focus of this mapping effort. While it would have been preferable to sample every mapped class, many of the sites were hazardous or inaccessible. Also, fires that occurred between the original imagery collection and the accuracy assessment imagery collection further complicated the issue. For example, the four accuracy assessment units that were located within areas mapped as *Salsola* sp. Provisional Alliance were all identified as having recently burned (and were identified as classes other than *Salsola* sp.). Funding and logistical constraints prevented the collection of the accuracy assessment imagery concurrently with the original imagery. Undersampled classes were retained in the original map despite the absence of accuracy assessment data because of their importance

for creating a map with full island coverage that can support biological resource management. Map users should consult Table 2 and Appendix S9 to understand the extent to which the accuracy of each class was assessed.

A final limitation is the applicability of our mapping approach and tools to other areas. The approach we used provides a structured rule set that integrates geospatial data inputs and fractional cover rules and is a substantial improvement over manual mapping techniques. However, it requires manual, site-specific adjustments to mapping rules to maintain consistent classification across the entire island. This is partly based on spatial variability of vegetation assemblages, physiography and soil background, as well as variations in image spectral-radiometric characteristics, mostly related to differential solar illumination.

5 | CONCLUSION

The fine-scale (Level 1) map of individual plants, patches of plant growth forms and land cover types, provided the basis for the community-level vegetation map (Level 2). Both levels of maps were refined through visual image interpretation and manual editing, but only the Level 2 map was subject to accuracy assessment at this time due to time and budget constraints. Assessment of the Level 1 map generated through this project would help explain how its accuracy influences the reliability of the Level 2 map.

With additional field work to establish the accuracy of the Level 1 map, it has potential to be used for vegetation monitoring in support of adaptive management by assessing rates and patterns of shrubland recovery. A multi-temporal analysis could be utilized for mapping and tracking changes of shrub cover fractions, while also evaluating how reliably species-level shrub cover can be estimated.

Optimal timing of future aerial surveys may provide some improvements in semi-automated tree species detection in high-relief terrain. Surveying additional trees using a combination of aerial imagery captured using unmanned aerial systems and field surveys would provide valuable species-level information.

Utilization of remote sensing imagery coupled with appropriate field-derived data provides an efficient and reasonably accurate means of mapping vegetation communities over broad spatial scales (Xie, Sha, & Yu, 2008). Object-based image analysis classification of high spatial resolution imagery for mapping and monitoring vegetation communities shows great promise. The methods employed in this study present a novel approach to improving the accuracy of semi-automated vegetation community mapping by combining the strengths of object-based image analysis contextual hierarchies that naturally occur throughout the environment, and structural vegetation data derived from digital surface models. Further, the methodology employed in this study has broader applicability in mapping vegetation communities in southern California and elsewhere.

ACKNOWLEDGEMENTS

Project success depended upon collaboration and support from several people and organizations. NEOS Ltd. captured and provided aerial VHSR and UHSR imagery for vegetation mapping and accuracy assessment. We wish to thank the following for their co-operation during this project: Lloyd Coulter, Alyson Scurlock, Gavin Schag, Melissa Booker, Emma Havstad, Kathryn Yeh, Dawn Lawson, Nicole Desnoyer, Susan Meiman, Sienna Hiebert, Lauren Garstka, Hector Elias Justiniani, and Cristiano Giovando. Special thanks to Jarlath O'Neil-Dunne for providing expert guidance regarding OBIA strategies for incorporating species cover rules.

AUTHOR CONTRIBUTIONS

JO, JL, LB, KO and BM provided input on the classification system and logistical support. AL performed image post-processing. KU, KW, DS, JO, RS and LB collected field data. KU, RS and DS developed the image processing methods. KU, KW and RS performed the mapping work. KA and KW analyzed the results. DS provided project supervision. KU wrote the paper with input from all authors.

DATA AVAILABILITY STATEMENT

The relevé and rapid assessment data sets are stored in the California Native Plant Society's vegetation database, and are available upon request. Other data sets associated with this study can be obtained by contacting the corresponding author.

ORCID

Kellie A. Uyeda  <https://orcid.org/0000-0001-7043-3870>

Douglas A. Stow  <https://orcid.org/0000-0001-5246-7073>

REFERENCES

- Baldwin, B. G., Goldman, D. H., Keil, D. J., Patterson, R., Rosatti, T. J., & Wilken, D. H. (2012). *The Jepson Manual: Vascular plants of California*. Berkeley, CA: University of California Press.
- Bitterroot Restoration Inc. (2002). Wetland Delineation and Endangered Species Surveys on Naval Auxiliary Landing Field San Clemente Island. Naval Facilities Engineering Command Southwest, U.S. Navy.
- Blaschke, T., Hay, G. J., Kelly, M., Lang, S., Hofmann, P., Addink, E., ... Tiede, D. (2014). Geographic object-based image analysis - Towards a new paradigm. *ISPRS Journal of Photogrammetry and Remote Sensing*, 87, 180–191. <https://doi.org/10.1016/j.isprsjprs.2013.09.014>
- Bork, E. W., & Su, J. G. (2007). Integrating LIDAR data and multispectral imagery for enhanced classification of rangeland vegetation: A meta analysis. *Remote Sensing of Environment*, 111, 11–24. <https://doi.org/10.1016/j.rse.2007.03.011>
- Chadwick, D. B., Ayers, J., Wild, W., Young, A., Melville, K., Statom, N., ... Flick, R. (2016). *San Clemente Island Baseline LiDAR Mapping: Final report*. San Diego, CA: SSC Pacific.
- Clark, M. L., & Kilham, N. E. (2016). Mapping of land cover in northern California with simulated hyperspectral satellite imagery. *ISPRS Journal of Photogrammetry and Remote Sensing*, 119, 228–245. <https://doi.org/10.1016/j.isprsjprs.2016.06.007>
- Corbane, C., Lang, S., Pipkins, K., Alleaume, S., Deshayes, M., García Millán, V. E., ... Michael, F. (2015). Remote sensing for mapping natural habitats and their conservation status - New opportunities and challenges. *International Journal of Applied Earth Observation*



- and *Geoinformation*, 37, 7–16. <https://doi.org/10.1016/j.jag.2014.11.005>
- Dobrowski, S. Z., Safford, H. D., Cheng, Y. B., & Ustin, S. L. (2008). Mapping mountain vegetation using species distribution modeling, image-based texture analysis, and object-based classification. *Applied Vegetation Science*, 11, 499–508.
- Eldridge, D. J., Bowker, M. A., Maestre, F. T., Roger, E., Reynolds, J. F., & Whitford, W. G. (2011). Impacts of shrub encroachment on ecosystem structure and functioning: Towards a global synthesis. *Ecology Letters*, 14, 709–722. <https://doi.org/10.1111/j.1461-0248.2011.01630.x>
- Faber-Langendoen, D., Keeler-Wolf, T., Meidinger, D., Tart, D., Josse, C., Navarro, G., ... Comer, P. (2014). EcoVeg : A new approach to vegetation description and classification. *Ecological Monographs*, 84, 533–561.
- Freeman, M. P., Stow, D., & Roberts, D. (2016). Object-based image mapping of conifer tree mortality in San Diego County based on Multitemporal Aerial Ortho-imagery. *Photogrammetric Engineering & Remote Sensing*, 82, 571–580. <https://doi.org/10.14358/PERS.82.7.571>
- Hamada, Y., Stow, D. A., & Roberts, D. A. (2011). Estimating life-form cover fractions in California sage scrub communities using multi-spectral remote sensing. *Remote Sensing of Environment*, 115, 3056–3068. <https://doi.org/10.1016/j.rse.2011.06.008>
- Hellesen, T., & Matikainen, L. (2013). An object-based approach for mapping shrub and tree cover on grassland habitats by use of LiDAR and CIR orthoimages. *Remote Sensing*, 5, 558–583. <https://doi.org/10.3390/rs5020558>
- Hiebert, S. R., Durzi, S., Garstka, L., & Zink, T. A. (2017). *San Clemente Island Native Habitat Restoration Program 2017 Annual Report*. Prepared for US Army Corps of Engineers.
- Hulet, A., Roundy, B. A., Petersen, S. L., Jensen, R. R., & Bunting, S. C. (2014). Cover estimations using object-based image analysis rule sets developed across multiple scales in pinyon-juniper woodlands. *Rangeland Ecology and Management*, 67, 318–327. <https://doi.org/10.2111/REM-D-12-00154.1>
- Jensen, J. R. (2007). *Remote sensing of the environment: An earth resource perspective*. Upper Saddle River, NJ: Pearson Prentice Hall.
- Junak, S., Knapp, D., Haller, J., Philbrick, R., Schoenherr, A., & Keeler-Wolf, T. (2007). The California Channel Islands. In M. Barbour, T. Keeler-Wolf, & A. Schoenherr (Eds.), *Terrestrial vegetation of California* (pp. 229–252). Berkeley, CA: University of California Press.
- Keegan, D. R., Coblentz, B. E., & Winchell, C. S. (1994). Feral goat eradication on San Clemente Island, California. *Wildlife Society Bulletin*, 22, 56–61.
- Laliberte, A. S., Rango, A., Havstad, K. M., Paris, J. F., Beck, R. F., McNeely, R., & Gonzalez, A. L. (2004). Object-oriented image analysis for mapping shrub encroachment from 1937 to 2003 in southern New Mexico. *Remote Sensing of Environment*, 93, 198–210. <https://doi.org/10.1016/j.rse.2004.07.011>
- Meiman, S., Munoz, S. A., DeLeon, E. E., Sandstrom, B., Nefas, S., & Bridges, A. S. (2017). *Surveys of Bell's sparrow habitat on San Clemente Island 2013–2016*. San Diego, CA: Institute for Wildlife Studies.
- Melville, K. W., Lenain, L., Cayan, D. R., Kahru, M., Kleissl, J. P., Linden, P. F., & Statom, N. M. (2016). The modular aerial sensing system. *Journal of Atmospheric and Oceanic Technology*, 33, 1169–1184. <https://doi.org/10.1175/JTECH-D-15-0067.1>
- Millington, A. C., & Alexander, R. W. (2000). Vegetation mapping in the last three decades of the twentieth century. In R. Alexander, & A. C. Millington (Eds.), *Vegetation mapping: From patch to planet* (pp. 321–331). Chichester, NY: John Wiley and Sons, LTD.
- O'Neil-Dunne, J. P. M., MacFaden, S. W., Royar, A. R., & Pelletier, K. C. (2013). An object-based system for LiDAR data fusion and feature extraction. *Geocarto International*, 28, 227–242. <https://doi.org/10.1080/10106049.2012.689015>
- Paudel, S., Benavides, J. C., Macdonald, B., Longcore, T., Wilson, G. W. T., & Loss, S. R. (2017). Determinants of native and non-native plant community structure on an oceanic island. *Ecosphere*, 8, 9. <https://doi.org/10.1002/ecs2.1927>
- Rapinel, S., Rossignol, N., Hubert-Moy, L., Bouzillé, J. B., & Bonis, A. (2018). Mapping grassland plant communities using a fuzzy approach to address floristic and spectral uncertainty. *Applied Vegetation Science*, 21, 678–693. <https://doi.org/10.1111/avsc.12396>
- Raven, P. H. (1963). A flora of San Clemente Island, California. *Aliso*, 5, 289–347.
- Sawyer, J. O., Keeler-Wolf, T., & Evens, J. M. (2009). *A manual of California vegetation*, 2nd ed. Sacramento, CA: California Native Plant Society.
- Schoenherr, A. A., Feldmeth, C. R., & Emerson, M. J. (2003). *Natural history of the islands of California*. Berkeley, CA: Univ of California Press.
- Snavely, R., Uyeda, K., Stow, D., O'Leary, J., & Lambert, J. (2019). Mapping vegetation community types in a highly-disturbed landscape: Integrating hierarchical object-based image analysis with lidar-derived canopy height data. *International Journal of Remote Sensing*, 40, 4384–4400. <https://doi.org/10.1080/01431161.2018.1562588>
- Sproul, F., Keeler-Wolf, T., Gordon-Reedy, P., Dunn, J., Klein, A., & Harper, K. (2011). *Vegetation Classification Manual for Western San Diego County*. Prepared for San Diego Association of Governments, San Diego, CA, USA. https://sdmmp.com/upload/projects/20160330_2357_94.pdf. Accessed June 18, 2018.
- Stahl, J. T., Gunther, J. P., Desnoyers, N. J., Bridges, A. S., & Garcelon, D. K. (2011). *San Clemente Loggerhead Shrike Monitoring Program Draft Annual Report–2010*. San Diego, CA: U.S. Navy, Environmental Department, Naval Facilities Engineering Command Southwest.
- Stohlgren, T. J., Chong, G. W., Kalkhan, M. A., & Schell, L. D. (1997). Multiscale sampling of plant diversity: Effects of minimum mapping unit size. *Ecological Applications*, 7, 1064–1074.
- Stout, D., Buck-Diaz, J., Taylor, S., & Evens, J. (2013). *Vegetation Mapping and Accuracy Assessment Report for Carrizo Plain National Monument*. Prepared by California Native Plant Society, Vegetation Program. <https://www.cnps.org/wp-content/uploads/2018/04/carrizo-mapping-report-2013.pdf>. Accessed June 18, 2018.
- Su, Y., Guo, Q., Fry, D. L., Collins, B. M., Kelly, M., Flanagan, J. P., & Battles, J. J. (2016). A vegetation mapping strategy for conifer forests by combining airborne LiDAR data and aerial imagery. *Canadian Journal of Remote Sensing*, 42, 1–15. <https://doi.org/10.1080/07038992.2016.1131114>
- Sward, W. L. & Cohen, R. H. (1980). *Plant Community Analysis of San Clemente Island*. Draft manuscript.
- Thorne, J., Kennedy, J., Quinn, J., McCoy, M., Keeler-Wolf, T., & Menke, J. (2004). A vegetation map of Napa County using the manual of California vegetation classification and its comparison to other digital vegetation maps. *Madroño*, 51, 343–363.
- Tierra Data Inc. (2011). *San Clemente Island Vegetation Condition and Trend Analysis, 2010*. San Diego, CA: Southwest Division U.S. Naval Facilities Engineering Command
- Tierra Data Inc. (2013). *Integrated natural resources management plan*. Escondido, CA: Naval Base Coronado, Natural Resources Office. http://tierradata.com/sci/wp-content/uploads/2012/10/SCIINRMP_PublicDraft_INRMP_021113.pdf
- Ullerud, H. A., Bryn, A., Halvorsen, R., & Hemsing, L. Ø. (2018). Consistency in land cover mapping: Influence of fieldworkers, spatial scale and classification system. *Applied Vegetation Science*, 21, 278–288.
- Uyeda, K. A., Stow, D. A., O'Leary, J. F., Schmidt, I. T., & Riggan, P. J. (2016). Spatial variation of fuel loading within varying aged stands of chaparral. *Applied Vegetation Science*, 19, 267–279. <https://doi.org/10.1111/avsc.12209>
- Westman, W. E., & O'Leary, J. F. (1986). Measures of resilience: The response of coastal sage scrub to fire. *Vegetatio*, 65, 179–189. <https://doi.org/10.1007/BF00044818>
- Woodcock, C. E., & Gopal, S. (2000). Fuzzy set theory and thematic maps: Accuracy assessment and area estimation. *International Journal of Geographical Information Science*, 14, 153–172. <https://doi.org/10.1080/136588100240895>

- Wylie, D. (2012). *Vegetation Change on San Clemente Island Following Removal of Feral Herbivores*. Master's thesis, San Diego State University.
- Xie, Y., Sha, Z., & Yu, M. (2008). Remote sensing imagery in vegetation mapping: A review. *Journal of Plant Ecology*, 1, 9–23. <https://doi.org/10.1093/jpe/rtm005>
- Yu, Q., Gong, P., Clinton, N., Biging, G., Kelly, M., & Schirokauer, D. (2006). Object-based detailed vegetation classification with airborne high spatial resolution remote sensing imagery. *Photogrammetric Engineering and Remote Sensing*, 72, 799–811. <https://doi.org/10.14358/PERS.72.7.799>
- Zhang, C., Xie, Z., & Selch, D. (2013). Fusing lidar and digital aerial photography for object-based forest mapping in the Florida Everglades. *Giscience and Remote Sensing*, 50, 562–573. <https://doi.org/10.1080/15481603.2013.836807>

SUPPORTING INFORMATION

Additional supporting information may be found online in the Supporting Information section.

Appendix S1. Vegetation community categories used in the mapping effort

Appendix S2. San Clemente Island vegetation mapping key

Appendix S3. Raster products used for vegetation classification and accuracy assessment

Appendix S4. Vector products used for vegetation classification

Appendix S5. Vector products used in rule set calibration

Appendix S6. Detailed lidar processing methods

Appendix S7. Algorithms used within the eCognition rule set to conduct image classification

Appendix S8. Image object features used as part of the rule set within eCognition to conduct image classification

Appendix S9. Areal coverage of vegetation communities for SCI based on image-based mapping procedures

Appendix S10. Fuzzy accuracy assessment

Appendix S11. Accuracy assessment error matrix showing only reference data mapped with high confidence.

Appendix S12. Accuracy assessment error matrix showing only reference data that fit entirely within a single mapping category

How to cite this article: Uyeda KA, Warkentin KK, Stow DA, et al. Vegetation mapping using hierarchical object-based image analysis applied to aerial imagery and lidar data. *Appl Veg Sci*. 2020;23:80–93. <https://doi.org/10.1111/avsc.12467>